

Entropically Patchy Particles

Greg van Anders,¹ N. Khalid Ahmed,¹ Ross Smith,² Michael Engel,¹ and Sharon C. Glotzer^{1,2}

¹Department of Chemical Engineering, University of Michigan, Ann Arbor, MI 48109-2136, USA

²Department of Materials Science and Engineering, University of Michigan, Ann Arbor, MI 48109-2136, USA

Directional entropic forces that cause particle alignment have recently been proposed in systems of hard polyhedra that order into crystals. Here we provide a means of quantifying these forces and find them to be of the order of a few $k_B T$. We show that these forces originate from “entropic patches,” which are features of particle shape that promote local dense packing. Using the notion of entropic patches, we engineer particle shape to target the assembly of specific crystal structures. We show that this procedure can be generalized as anisotropy dimensions, similar to those exploited for enthalpically patchy particles.

It is known since the work of Kirkwood on hard spheres [1] and Onsager on hard rods [2] that entropy can order hard particles. Recent studies have explored the role of entropy in ordering hard, convex shapes between the sphere and rod limits [3–20]. The role of shape in self-assembly has been reviewed recently in [21]. A general observation from many of these studies is that hard polyhedra align their facets at sufficiently high packing fractions (typically, greater than 50%). Based on this observation, Damasceno, et al. [13, 14] argued for the existence of “directional entropic forces” between hard particles. Due to these forces, spontaneous first order transitions were observed in computer simulation where particles aligned upon increasing packing fraction from a disordered fluid to colloidal quasicrystals, liquid crystals, and crystals with unit cells containing as many as 52 particles [13, 14].

Here we compute the directional entropic forces in hard particle systems, by introducing a potential of mean force and torque (PMFT). We show that the effective interaction strengths can be on the order of a few $k_B T$, putting them in a range that makes them an important consideration for self-assembly in experimental colloidal systems. We then show that directional entropic forces can be engineered through the systematic alteration of particle shape to target specific self-assembled structures. We conceptualize this shape engineering as the creation of “entropic patches,” in analogy with the engineering of enthalpic patches using chemical or other means introduced in [22] and reviewed in [23, 24]. In contrast to the charge, chemical, etc. mediation of the interaction between sticky patches on *enthalpically* patchy particles, attractive *entropic* patches are features in particle shape that promote dense packing. Finally, we demonstrate the generality of directional entropic forces as a design concept by introducing anisotropy dimensions [23] for entropic patchiness.

As a means of quantifying directional entropic forces, we examine a single pair of hard particles in a larger system of identical hard particles. Such a treatment was first given in the case of spheres by de Boer [25]; for aspherical particles, first steps were taken in this direction in [26, 27]. At constant volume and number of particles, the partition function of the system has the form

$$\mathcal{Z} = \int dq_{1,2} dQ_{1,2} [d\tilde{q}] [d\tilde{Q}], \quad (1)$$

where $\{q\}$ are the center of mass coordinates of the particles

and $\{Q\}$ are the particle orientations. We have identified the particle pair of interest with the labels 1 and 2. All other particles are indicated with a tilde. For axisymmetric particles (to which we restrict our consideration here for brevity, see [28] for the general case), the pair has only four rotational and translational degrees of freedom. If their centers of mass are separated by \tilde{q}_{12} , and their symmetry axes are $\hat{n}_{1,2}$, then those four degrees of freedom, written to be invariant under rotations of the whole system, are

$$\{R \equiv |\tilde{q}_{12}|, \phi_1 \equiv \hat{n}_1 \cdot \hat{q}_{12}, \phi_2 \equiv -\hat{n}_2 \cdot \hat{q}_{12}, \chi \equiv -\hat{n}_1 \cdot \hat{n}_2\}. \quad (2)$$

Fixing the values of these coordinates allows us to find F_2 , the effective (see, e.g., [29]) potential of mean force and torque (PMFT), from

$$\begin{aligned} \mathcal{Z} &= \int dR d\phi_1 d\phi_2 d\chi e^{-\beta F_2(R, \phi_1, \phi_2, \chi)} \\ &= \int dR d\phi_1 d\phi_2 d\chi J(R, \phi_1, \phi_2, \chi) \\ &\quad H(d(R, \phi_1, \phi_2, \chi)) e^{-\beta \tilde{F}(R, \phi_1, \phi_2, \chi)}. \end{aligned} \quad (3)$$

The Jacobian J is

$$J(R, \phi_1, \phi_2, \chi) = \frac{R^2}{\sqrt{1 - \chi^2 - \phi_1^2 - \phi_2^2 + 2\phi_1\phi_2\chi}}, \quad (4)$$

H is the Heaviside step function, and $d(R, \phi_1, \phi_2, \chi)$ is the minimum separation distance of the particle pair in their relative position and orientation, which is negative when the particles overlap, and positive when they do not. Note that if we were considering particles that interacted other than sterically, the Heaviside function would be replaced with the Boltzmann factor of the pair interaction energy. \tilde{F} is the Helmholtz free energy available to other particles in the system when the relative position and orientation of the pair is fixed. F_2 is then the free energy of the entire system, including the particle pair of interest and the remaining degrees of freedom, when the relative position and orientation of the pair are fixed. Equating the integrands and taking the logarithm of both sides gives the PMFT

$$\begin{aligned} \beta F_2(R, \phi_1, \phi_2, \chi) &= \beta \tilde{F}(R, \phi_1, \phi_2, \chi) \\ &\quad - \log(J(R, \phi_1, \phi_2, \chi) H(d(R, \phi_1, \phi_2, \chi))). \end{aligned} \quad (5)$$



	$\psi = \frac{61}{64}$	$\psi = \frac{63}{64}$
		
$R = 0.3$	3.48 ± 0.05	1.16 ± 0.01
$R = 0.4$	3.64 ± 0.06	2.39 ± 0.03

TABLE I. Angular dependence of the PMFT. Figures are height of the potential in $k_B T$ above the global minimum for slice of the potential with $\psi \equiv \phi_1 = \phi_2 = \chi$ fixed. Although the angular differences are small (perfect alignment is $\psi = 1$), the effective interaction varies by more than $2 k_B T$ over this angular range at small separations, indicating that the penalty for small misalignment is significant. Inset particle images illustrate the relative orientations shown.

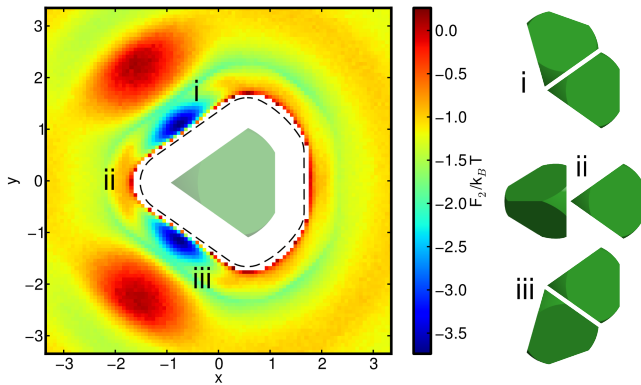


FIG. 1. The PMFT exhibits strong directionality of entropic forces between particles, shown here through a slice of the force component of the PMFT with angular directions integrated out. It displays a force towards the tetrahedral coordination (i) and (iii) of tetrahedrally faceted spheres, compared with non-tetrahedral coordination (ii), here shown for a fluid at a density of 50%. The dashed curve shows the location of the steric exclusion boundary for the center of mass of the second particle around the inset particle.

The mean directional entropic forces and torques responsible for particle alignment are encoded in the PMFT (5). If we were to label just a single pair of particles in a system of colloidal particles subject to thermal (Brownian) motion, we would infer that the force and torque on particle 1 due to particle 2 would be given by

$$\begin{aligned} \vec{F}_1 &= -\hat{r}_{12} \frac{\partial F_2}{\partial R} - (\hat{n}_1 - \hat{r}_{12} \phi_1) \frac{\partial F_2}{\partial \phi_1} - (\hat{n}_2 + \hat{r}_{12} \phi_2) \frac{\partial F_2}{\partial \phi_2}, \\ \vec{T}_1 &= -\hat{r}_{12} \times \hat{n}_1 \frac{\partial F_2}{\partial \phi_1} + \hat{n}_2 \times \hat{n}_1 \frac{\partial F_2}{\partial \chi}. \end{aligned} \quad (6)$$

These equations specify the forces and torques we would expect to measure if, e.g., we grabbed a particle pair in a system of hard colloids using optical tweezers and attempted to pull them apart.

As a simple example of the role of the PMFT in aligning particles, consider a particle obtained from a sphere of radius

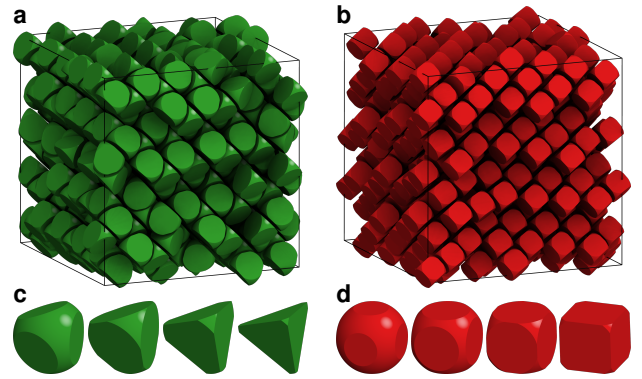


FIG. 2. Self-assembled structures of faceted spheres obtained in MC simulation by designing particle shape. Panel (a) shows a diamond lattice obtained by giving a particle tetrahedrally coordinated facets as in (c). Panel (b) shows a simple cubic lattice, obtained by giving particles cubically coordinated facets as in (d).

r by cutting away the part of the sphere that intersects the half space \mathbb{R}^3 for which $z/r > \alpha$ to create a singly faceted sphere. We performed MC simulations of systems of 1000 such particles with $\alpha = 0.01$ (nearly hemispherical) at fixed volume. In table I we show the role of the PMFT in generating entropic torques that align particle facets in this system at a density of 50%. We find the potential difference between different particle orientations at fixed separation distance is of the order of a few $k_B T$, giving rise to entropic torques strongly favoring alignment. In Fig. 1 we show the role of the PMFT in generating directional entropic forces that cause particles to have positional correlation at facets. We plot the force component of the PMFT for tetrahedrally faceted spherical particles as a function of the Cartesian components of the separation vector of the particles in the frame of one of the particles. The plot shows potential minima in which the particle pairs have tetrahedral coordination (i) and (iii), compared with, e.g., facet-edge configurations (ii); differences are on the order of a few $k_B T$. In both cases, the role of facets as entropic “patches” that favor facet alignment is evident.

Entropic patches can be used to design particles for the purpose of self-assembling specific structures. In particular, that the forces are on the order of a few $k_B T$ puts them in the range that is important for self-assembly. Indeed, experiments demonstrate that directional entropic forces can dominate assembly in the presence of weak enthalpic interactions [15, 30, 31]. As an example, we consider targeting the assembly of a (tetrahedrally-coordinated) diamond lattice by tetrahedrally faceting spheres; i.e. we “slice” four equal sized facets into the sphere at the locations of the faces of a regular tetrahedron. If we consider a facetting amount of 0 to be a perfect sphere, and 1 to be a perfect tetrahedron, then at a facetting amount of 0.6 the particles self-assemble a diamond lattice in MC simulation at a packing fraction of 60% as shown in Fig. 2a. Similarly, if we apply cubic facetting to a sphere by denoting a perfect sphere as 0 and a perfect cube as 1, simple cubic lattices (Fig. 2b) assemble at an amount of

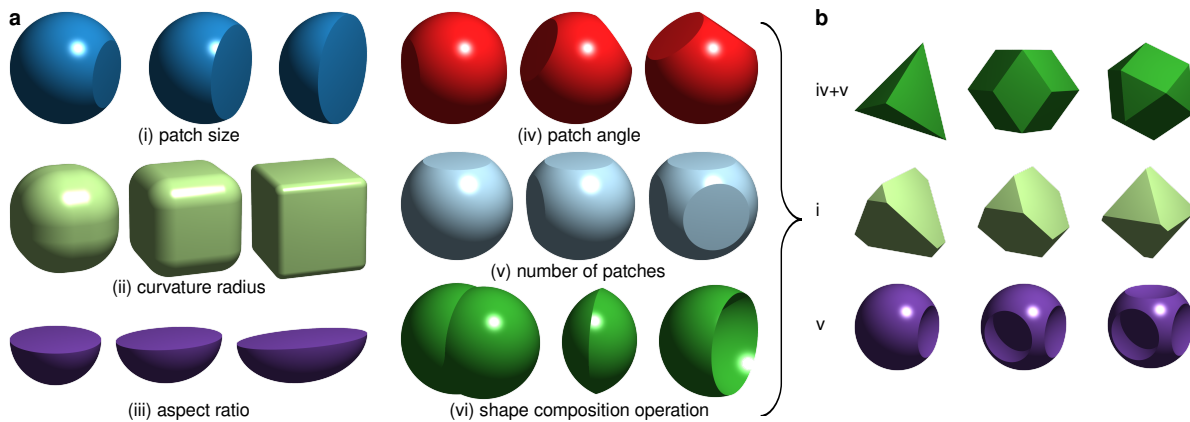


FIG. 3. (a) The creation and altering of entropic patches can be conceptualized as anisotropy dimensions: four that are realized continuously are (i) patch size, (ii) curvature radius, (iii) aspect ratio, and (iv) patch angle; two that are realized discretely are (v) number of patches, and (vi) shape composition operation. (b) Various anisotropy dimensions from panel (a) can be combined to recover familiar shapes. From top to bottom: combining the anisotropy dimensions of patch angle and patch number (iv and v from panel a) recovers various polyhedra, here a tetrahedron, a rhombicdodecahedron, and a cuboctahedron; changing the patch size (i from panel a) by combining two tetrahedra of different sizes through intersection yields various truncated tetrahedra; by changing the patch number (v from panel a) of a sphere that has been faceted with another sphere, various lock particles dimpled spheres can be realized.

0.6 or more in MC simulations at packing fractions of 54% or more. Phases for other facetting amounts are shown in Fig. 5.

The competition between the entropy available to a pair of particles in isolation from the rest of the system and the osmotic pressure of the rest of the system on the pair causing it to arrange more densely gives rise to the entropic ordering in Fig. 2. This competition is manifest in the two terms in (5). Here, $-\beta\tilde{F} = \tilde{S}$, the entropy available to the rest of the system for a fixed configuration of the particle pair. Locally, \tilde{S} is an increasing function of the volume available to the rest of the system, meaning the remainder of the system has an entropic preference for the dense packing of the pair. This term is of the order of the stress tensor in the system. In the infinite pressure limit, relevant for packing, this term dominates. However, for assembly, which occurs at finite pressures, both terms contribute, and it is this competition that can lead to a difference between dense packing and assembled structures, as has been noted in several recent studies [11, 13–15, 18].

Here we engineered particle shape to promote locally dense packing by facetting spheres, but there are many ways of altering particle shape to promote locally dense packing. The fact that directional entropic forces cause alignment of facets, thereby controlling the arrangement of particles in successive neighbor shells, is reminiscent of the angular specificity of interactions conceptualized as patchy particles in [22, 23]. The notion of (enthalpically) patchy particles provided a new means of conveying angular specificity to particle-particle interactions in a way that was previously only possible for molecules. Examples of patchy particles include Janus colloids [32–36], striped nanospheres [37] and nanorods, [38], and DNA-coated patchy particles [39], among many others (see the reviews [23, 24]). However, in contrast to the chemical or other patterning that leads to enthalpic patchiness, the angular specificity of interactions arises here solely due to en-

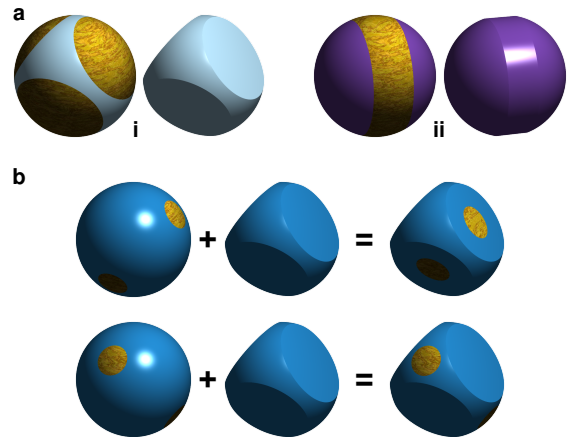


FIG. 4. (a) Many anisotropy dimensions for enthalpically patchy particles [23] have entropically patchy counterparts. Example traditional sticky patchy particles left (i) and (ii) with entropically patchy counterparts right (i) and (ii). (b) Enthalpic patches can be combined with entropic patches to enhance or inhibit entropic patchiness as shown schematically here. This can be obtained by using the same direction for both types of patches (left), or by using different directions for the entropic patches and the enthalpic patches (right).

tronic considerations that arise from particle shape. The features in shape that promote dense packing are, in effect, acting as “entropic patches” that cause preferential alignment. We introduce a design space for these entropic patches, as was done for enthalpic patches [23], through anisotropy dimensions (Fig. 3a). In contrast to traditional sticky patches, entropic patchiness is an emergent, effective concept that depends on packing fraction and on all geometric features that come within the characteristic length of the interaction at a given packing fraction. Such features may include, e.g.,

flat facets or other low curvature regions, and interlocking or “mating” features. Conversely, high curvature regions could be used to introduce repulsive patches.

Six examples of anisotropy dimensions are illustrated in Fig. 3a. Examples of continuous anisotropy dimensions include (i) patch size, (ii) curvature radius, (iii) aspect ratio, and (iv) patch angle. Examples of discrete anisotropy dimensions include (v) number of patches and (vi) shape composition operation. These anisotropy dimensions can be combined in different ways (Fig. 3b) to recover particles of various known shapes, e.g. polyhedra and dimpled lock-and-key colloids [40, 41]. We also note that many of these anisotropy dimensions map naturally to anisotropy dimensions introduced for enthalpically patchy particles [23]. Examples of enthalpically patchy particles and their entropically patchy analogues are shown in Fig. 4a.

When combined with traditional enthalpic patchiness, entropic patchiness greatly enlarges the already vast design space for new nano- and micron-scale building blocks. The formalism presented here allows the assessment of the relative strength of entropic driving forces for assembly when other forces also contribute. In experimental systems, particles are seldom solely hard [42]. However, the fact that the scale of interaction is on the order a few $k_B T$ at intermediate packing densities means that there might be a large class of systems in which electrostatic or other forces can be sufficiently controlled such that entropic patches supply the dominant force controlling their self-assembly, as was demonstrated recently in [30, 31]. Of course, as depicted in Fig. 4b, combining enthalpic patches with entropic patches, e.g. grafting DNA or other ligands to facets, should enhance the tendency for face-to-face alignment of particles. Such interplay of forces underlies bulk assemblies observed for naturally faceted nanoparticles [15].

Finally, we note that entropic patchiness does not require depletant molecules. The connection to depletion is discussed in a forthcoming paper [28].

We thank Daan Frenkel and Randall Kamien for discussions concerning the early literature. This material is based upon work supported by, or in part by, the U.S. Army Research Office under Grant Award No. W911NF-10-1-0518, the DOD/ASD(R&E) under Award No. N00244-09-1-0062.

Methods

To measure the potential of mean force (PMFT) we performed Monte Carlo (MC) simulations of fluids of 1000 hard faceted spheres at fixed volume. Results in Table I are for nearly hemispherical particles; the radius of the sphere was taken to be unity, and the distance from the facet to the center of the sphere was taken to be 0.01 to avoid numerical errors that would occur in our algorithms if the center of the sphere was taken to lie on the the facet. The PMFT was computed in a fluid at equilibrium by partitioning the four scalar quantities defining independent relative positions and orientations

into finite-size regions, and counting the relative frequency of observing a pair of particles in each region. Error bars are standard errors of the mean of independent runs of independently equilibrated systems.

Similarly, for Fig. 1 MC simulations of tetrahedrally faceted spheres were performed. The displacement between particles was computed in the coordinate frame of each particle, and possible relative positions were partitioned into finite-sized regions. The PMFT was computed by observing the relative frequency of observing a pair of particles in each region. The results show the average of several independent runs.

The MC method employed above, and for the results shown in Fig. 2 and Fig. 5 employed single particle moves for both translation and orientation. In all cases the simulation box was taken to be periodic and the volume fixed. However, for Fig. 2 and Fig. 5, the box was permitted to shear at fixed volume. In all cases, faceted spheres were approximated by polyhedra with 113 or more vertices, depending on the facetting amount, and overlaps were checked using the same implementation of the GJK algorithm [43] as used in [14].

In Fig. 5 we show the phases that self-assembled in MC simulations.

-
- [1] J. G. Kirkwood, *J. Chem. Phys.* **7**, 919 (1939).
 - [2] L. Onsager, *Ann. NY Acad. Sci.* **51**, 627 (1949).
 - [3] D. Frenkel, *J. Phys. Chem.* **91**, 4912 (1987).
 - [4] A. Stroobants, H. N. W. Lekkerkerker, and D. Frenkel, *Phys. Rev. A* **36**, 2929 (1987).
 - [5] T. Schilling, S. Pronk, B. Mulder, and D. Frenkel, *Phys. Rev. E* **71**, 036138 (2005).
 - [6] B. S. John, C. Juhlin, and F. A. Escobedo, *J. Chem. Phys.* **128**, 044909 (2008).
 - [7] A. Haji-Akbari, M. Engel, A. S. Keys, X. Zheng, R. G. Petschek, P. Palfy-Muhoray, and S. C. Glotzer, *Nature* **462**, 773 (2009).
 - [8] W. H. Evers, B. D. Nijs, L. Fillion, S. Castillo, M. Dijkstra, and D. Vanmaekelbergh, *Nano Lett.* **10**, 4235 (2010).
 - [9] U. Agarwal and F. A. Escobedo, *Nat. Mater.* **10**, 230 (2011).
 - [10] K. Zhao, R. Bruinsma, and T. G. Mason, *PNAS* **108**, 2684 (2011).
 - [11] A. Haji-Akbari, M. Engel, and S. C. Glotzer, *Phys. Rev. Lett.* **107**, 215702 (2011).
 - [12] L. Rossi, S. Sacanna, W. T. M. Irvine, P. M. Chaikin, D. J. Pine, and A. P. Philipse, *Soft Matter* **7**, 4139 (2011).
 - [13] P. F. Damasceno, M. Engel, and S. C. Glotzer, *ACS Nano* **6**, 609 (2012).
 - [14] P. F. Damasceno, M. Engel, and S. C. Glotzer, *Science* **337**, 453 (2012).
 - [15] J. Henzie, M. Grünwald, A. Widmer-Cooper, P. L. Geissler, and P. Yang, *Nat. Mater.* **11**, 131 (2012).
 - [16] R. Ni, A. P. Gantapara, J. de Graaf, R. van Roij, and M. Dijkstra, *Soft Matter* **8**, 8826 (2012).
 - [17] J. Zhang, Z. Luo, B. Martens, Z. Quan, A. Kumbhar, N. Porter, Y. Wang, D.-M. Smilgies, and J. Fang, *J. Am. Chem. Soc.* **134**, 14043 (2012).
 - [18] U. Agarwal and F. A. Escobedo, *J. Chem. Phys.* **137**, 024905 (2012).

- [19] F. Smalenburg, L. Filion, M. Marechal, and M. Dijkstra, PNAS **109**, 17886 (2012).
- [20] M. Marechal, A. Patti, M. Dennison, and M. Dijkstra, Phys. Rev. Lett. **108**, 206101 (2012).
- [21] L. Cademartiri, K. J. M. Bishop, P. W. Snyder, and G. A. Ozin, Phil. Trans. Royal Soc. A **370**, 2824 (2012).
- [22] Z. Zhang and S. C. Glotzer, Nano Lett. **4**, 1407 (2004).
- [23] S. C. Glotzer and M. J. Solomon, Nat. Mater. **6**, 557 (2007).
- [24] A. B. Pawar and I. Kretzschmar, Macromol. Rapid Comm. **31**, 150 (2010).
- [25] J. de Boer, Rep. Prog. Phys. **12**, 305 (1949).
- [26] G. H. A. Cole, Proc. Phys. Soc. **75**, 77 (1960).
- [27] C. Croxton and T. Osborn, Phys. Lett. A **55**, 415 (1975).
- [28] G. van Anders, N. K. Ahmed, M. Engel, and S. C. Glotzer, in preparation (2013).
- [29] C. N. Likos, Phys. Rep. **348**, 267 (2001).
- [30] K. L. Young, M. R. Jones, J. Zhang, R. J. Macfarlane, R. Esquivel-Sirvent, R. J. Nap, J. Wu, G. C. Schatz, B. Lee, and C. A. Mirkin, PNAS **109**, 2240 (2012).
- [31] X. Ye, C. Jun, M. Engel, J. A. Millan, W. Li, L. Qi, G. Xing, J. E. Collins, C. R. Kagan, J. Li, S. C. Glotzer, and C. B. Murray, Nat. Chem. in press (2013).
- [32] O. Cayre, V. N. Paunov, and O. D. Velev, J. Mater. Chem. **13**, 2445 (2003).
- [33] K-H. Roh, D. C. Martin, and J. Lahann, Nat. Mater. **4**, 759 (2005).
- [34] G. Zhang, D. Wang, and H. Möhwald, Nano Lett. **5**, 143 (2005).
- [35] J.-Q. Cui and I. Kretzschmar, Langmuir **22**, 8281 (2006).
- [36] L. Hong, S. Jiang, and S. Granick, Langmuir **22**, 9495 (2006).
- [37] A. M. Jackson, J. W. Myerson, and F. Stellacci, Nat. Mater. **3**, 330 (2004).
- [38] B. R. Martin, D. J. Dermody, B. D. Reiss, M. Fang, L. A. Lyon, M. J. Natan, and T. E. Mallouk, Adv. Mater. **11**, 1021 (1999).
- [39] Y. Wang, Y. Wang, D. R. Breed, V. N. Manoharan, L. Feng, A. D. Hollingsworth, M. Weck, and D. J. Pine, Nature **491**, 51 (2012).
- [40] G. Odriozola, F. Jimenez-Angeles, and M. Lozada-Cassou, J. Chem. Phys. **129**, 111101 (2008).
- [41] S. Sacanna, W. T. M. Irvine, P. M. Chaikin, and D. Pine, Nature **464**, 575 (2010).
- [42] C. P. Royall, W. C. K. Poon, and E. R. Weeks, Soft Matter **9**, 17 (2013).
- [43] E. Gilbert, D. Johnson, and S. Keerthi, IEEE J. Rob. Auto. **4**, 193 (1988).

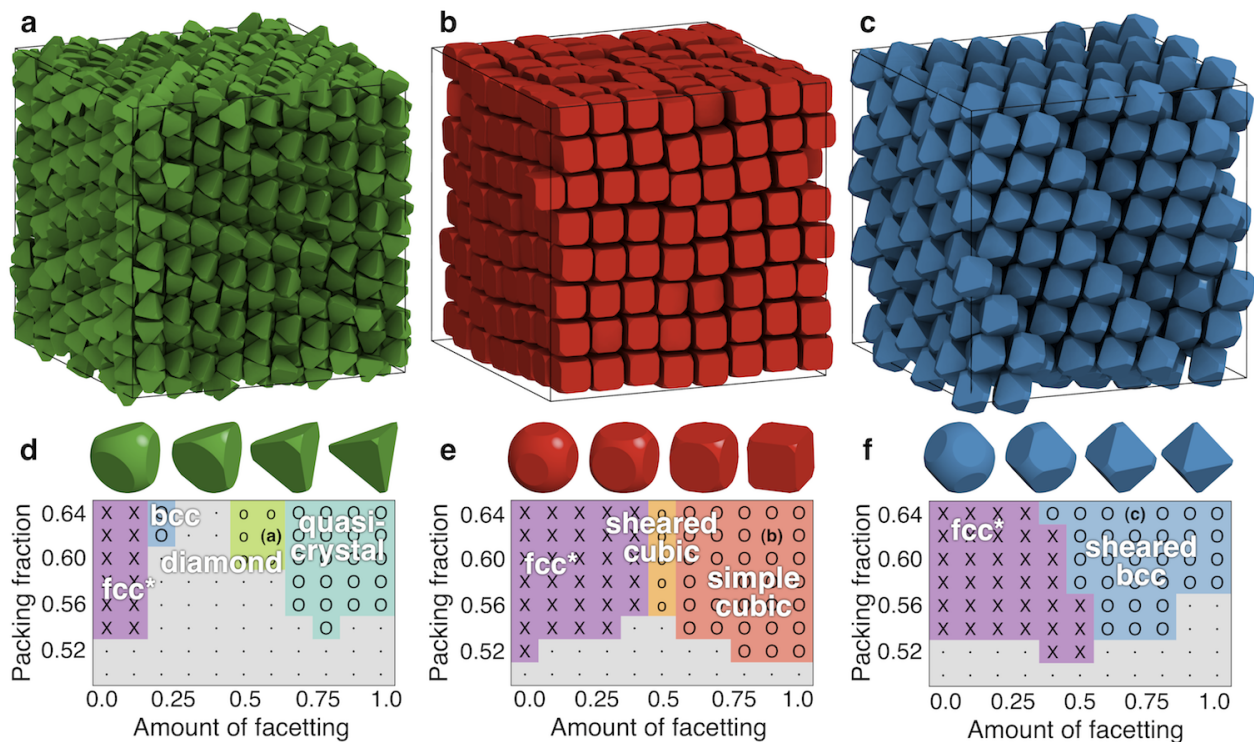


FIG. 5. Self-assembled phases of entropically patchy hard spheres. We explore the effect of the anisotropy dimensions of facetting number, angle, and size from Fig. 3. Sufficiently strong entropic patches require at least some facet alignment, which in turn determines the final crystal structure.